Int J Adv Manuf Technol (2017) 89:561–579
DOI 10.1007/s00170-016-8981-x

ORIGINAL ARTICLE

An approach of comprehensive error modeling and accuracy allocation for the improvement of reliability and optimization of cost of a multi-axis NC machine tool

Ziling Zhang[1] · Zhifeng Liu[1] · Qiang Cheng[1] · Yin Qi[2] · Ligang Cai[1]

Received: 28 January 2016 / Accepted: 25 May 2016 / Published online: 5 July 2016

Abstract Machining accuracy is critical for the quality and performance of a mechanical product, and the reliability of a multi-axis NC machine tool reflects the ability to reach and maintain the required machining accuracy. The objective of this study is to propose a general methodology that will simultaneously consider geometric errors and thermal-induced errors to allocate the geometric accuracy of components, for improving machining accuracy reliability under certain design requirements. The multi-body system (MBS) theory was applied to develop a comprehensive volumetric error model, showing the coupling relationship between the individual errors of the components of this machine tool and their volumetric accuracy. Additionally, a thermal error model was established based on the neural fuzzy control theory and was compared to the common thermal error modeling method called BP neural network. Based on the traditional cost model and the reliability analysis model, a geometric error-cost model and a geometric error-reliability model were established, taking the weighted function principle into consideration. Then, an allocation approach of the geometric errors, for optimizing total cost (manufacture and QLF) and reliability, subject to the geometrical and operational constraints of the machine tool, was proposed and formulated into a mathematical model, in order to perform the optimization process of accuracy allocation by using the advanced NSGA-II algorithm. A case study was also performed in a five-axis machine tool, and the traditional NSGA algorithm was used for comparison. The optimization results for the five-axis machining center showed that the proposed approach is effective and able to perform the optimization of geometric accuracy and improve the machining accuracy and the reliability of the machine tool.

Keywords Thermal-induced errors · Reliability · Cost · Machining accuracy · Machine tool

1 Introduction

NC machine tools are widely used throughout the manufacturing industry, and their machining accuracy is critical to the dimensional accuracy of parts [5]. In general, NC machine tool errors can be classified into four types: geometric errors of machine components and structures, errors induced by thermal distortions, deflection errors caused by cutting forces, and other errors, such as those caused by servo motors, errors of machine axes rotation, or numerical control interpolation algorithmic errors [20]. The geometric errors, which include pitch error in lead screws, straightness error in guideways, angular error in machine slides, and orthogonality error between the machine axes, account for 30 % of the machining accuracy [2, 22]. Hence, it should be taken into special consideration during the configuration and allocation of appropriate dimensional errors in the design of machine tools, in order to provide satisfactory machining accuracy and cost-effective geometric accuracy allocation, which is an intractable problem for machine tool manufacturers. Considering that machine tools are usually made by several assembly parts, the dimensional and geometric variations of each part have to be specified by tolerances which guarantee a certain level of quality, in terms of satisfying

✉ Zhifeng Liu
lzfbjut@gmail.com

[1] Beijing Key Laboratory of Advanced Manufacturing Technology, Beijing University of Technology, Beijing 100124, China

[2] Yingtan Technical School, Yingtan, Jiangxi 335000, China

functional requirements [36]. As a result, accuracy design of machine tools is a problem of allocation of these geometric errors and such problem can be divided into two aspects: one is how to establish a geometric error model to obtain the coupling relationship between the individual errors of the components of the machine tool and its volumetric accuracy, while the other is to perform the geometric error allocation.

The foundation of accuracy design is accuracy modeling, and a model that explains how individual error of the components of a machine affects its volumetric accuracy is of critical value to the accuracy distribution approach, which comprises one aspect of importance of this paper. Following a literature review, it is evident that many researches have been focused on modeling of multi-axis machine tools to find out the resultant error of individual components in relation to tool and work-piece point deviation. The development of various modeling methods has been performed for many years, and some of the most important methods include the matrix translation method, error matrix method, rigid body kinematic, D-H method, homogeneous transformation matrices (HTMs), and modeling methods based on the multi-body system kinematics theory [1, 11, 13, 17, 23, 30, 32, 37]. In 1977, Schultschick first formulated a volumetric error model for a three-axis jig boring machine using a vector chain expression [33]. Ferreira and Liu described a general method for modeling the geometric error of a three-axis machine based on the homogeneous coordinate transformation method [16]. In 1991, Kim and Kim extended Schultschik's work by modeling the geometric errors in the workspace base on rigid body kinematics to predict the accuracy of three-axis machines with the assumption of small-angle approximation [24]. In 1992, Chen et al. addressed an approach for compensation of non-rigid body kinematic effect on a machining center [3]. In recent years, the multi-body system (MBS) theory is used to provide a unique systematic approach and many investigators have carried out error modeling research for complicated machinery system using MBS [26, 48, 51, 53]. In 2002, Fan et al. proposed the kinematics of MBS by adding movement error items and positioning error items and then developed a universal way of how to make a kinematics model of NC machine tools [14]. In 2002, Liu presented an error model for the thermal errors in machining centers together with the corresponding compensation method [27]. In 2003, Wang et al. proposed a model for the geometric error of the five-axis CNC machine tools based on MBS and developed the key technique for the compensation-identifying geometric error parameters [42]. In 2007, Ding et al. investigated the methodology of accuracy design and constructed the accuracy model including 21 basic geometric error components using the MBS [9]. In 2015, Cheng et al. constructed the volumetric error model to track and compensate the effects of the errors during the operation of the machine by applying the MBS theory [4].

Accuracy allocation, as the other aspect of importance of this paper, is to obtain the accuracy of updated and maintained parts according to the presetting accuracy of machine tools and let the accuracy of parts reach optimal in certain meaning [19]. In fact, this is actually a problem of structural optimization and its aim is to obtain the optimum solution under specified limitations and limited resources [6]. To date, there are many researchers focusing their attention on accuracy allocation of structural designs and some allocation models have been developed in the field of naval engineering, measuring machines, robotics, military weapons, and instrumentation [28, 40, 41, 45, 52]. However, the research on accuracy allocation of machine tools is primarily targeting at the parallel machine tool development [29, 43, 46], and a systemic approach for accuracy allocation of multi-axis machine tools has not been developed yet, with limited studies focusing on the field of machine tool design. In 1994, Dorndorf et al. proposed an error allocation approach to optimize allocation of manufacturing and assembly tolerances along with specifying the operating conditions, and in order to determine the optimal level for these errors of a two-axis machine tool [11], it is regardless of quality loss. In 2013, Yu et al. proposed a geometric error propagation model and reliability approximately model by response surface method with error samples and improved the functions of machine tools by optimization of the sensitivity with the single-failure model [49]. In 2014, Cheng et al. addressed an optimal model for accuracy allocation of machine tools, based on the MBS theory and reliability-based design optimization [4]. In 2015, Cai et al. proposed an accuracy distribution method for machine tools with multiple failure modes, by applying the AFOSM theory [7]. Krishna and Rao used the scatter search method to simultaneously allocate both the design and manufacturing tolerances, based on a minimum total manufacturing cost [25]. Huang et al. established a sequential linear optimization model based on the process capabilities [18]. Jin et al. presented a tolerance design approach for automotive parts at an early design stage [21]. The above researches did not take the influence of the accuracy to the total cost (manufacturing cost and quality loss) into consideration or neglected the reliability of machine tools. As a result, there is a continuous effort in seeking a geometric error-cost model and a geometric error-reliability model to develop a general accuracy allocation approach that will simultaneously consider cost and reliability to allocate

the geometric accuracy of components for improving machining accuracy under certain design requirements.

The rest of this paper will be configured as follows. In Section 2, a comprehensive error model was established based on the MBS and neural fuzzy control theory. In Section 3, a geometric error-cost model and a geometric error-reliability model were developed. By combining these two models, a general accuracy allocation approach that simultaneously considers cost and reliability is proposed and it is formulated into a mathematical model, in order to allocate geometric accuracy of components for improving machining accuracy reliability and optimizing cost under certain design requirements. A case study was also performed in a five-axis machine tool as an example in Section 4. It is followed by conclusions and recommendations for future work.

2 Error modeling of NC machine tools

In this paper, an XKH800 five-axis machining center was used to analyze geometric errors and the geometric/kinematic error model was developed. This machining center is designed for leaf blade machining and is comprised by three linear axes (*X*, *Y*, *Z*) and two rotary axes (*A*, *B*). The three-dimensional model of the XKH800 center is presented in Fig. 1a. Taking the error factors and coupling relations of the various parts into consideration, the five-axis machine tool can be abstracted into a topology framework, as shown in Fig. 1b, and each body in the topology framework corresponds to each of the three-dimensional model. Also, the main parameters of the machine tool are listed in Table 1. The MBS theory was applied to establish a machine tool geometric/kinematic error model, showing the relation between the individual errors of the components of this machine tool, and its volumetric accuracy is critical for the allocation of standard deviation for the geometric parameter errors. Due to limited space, a full description of the complete analysis was avoided and only the most important findings of the characteristic matrices of the five-axis NC machining center were described, as follows:

It is supposed that $\boldsymbol{K}_{\boldsymbol{A_iA_{i+1}P}}$, $K_{\boldsymbol{A_iA_{i+1}S}}$, $\Delta K_{\boldsymbol{A_iA_{i+1}P}}$, and $\Delta K_{\boldsymbol{A_iA_{i+1}S}}$ refer to the ideal static characteristic matrix, the ideal motion characteristic matrix, the static error characteristic matrix, and the kinematic error characteristic matrix of the adjacent body, respectively.

Taking the spindle as example, the body kinematic error homogeneous transformation matrix can be given as follows:

$$\Delta K_{A_3A_4S} = \begin{pmatrix} 1 & -\Delta\gamma_\psi & \Delta\beta_\psi & \Delta x_\psi \\ \Delta\gamma_\psi & 1 & -\Delta\alpha_\psi & \Delta y_\psi \\ -\Delta\beta_\psi & \Delta\alpha_\psi & 1 & \Delta z_\psi \\ 0 & 0 & 0 & 1 \end{pmatrix} \tag{1}$$

Equation (1) contains three parts: the geometric errors, the thermal-induced errors, and the cutting force-induced errors, and so, it can be rewritten as

$$\Delta\boldsymbol{K}_{\boldsymbol{A_3A_4S}} = \begin{pmatrix} 1 & -\left(\Delta\gamma_\psi^g + \Delta\gamma_\psi^t + \Delta\gamma_\psi^f\right) & \Delta\beta_\psi^g + \Delta\beta_\psi^t + \Delta\beta_\psi^f & \Delta x_\psi^g + \Delta x_\psi^t + \Delta x_\psi^f \\ \Delta\gamma_\psi^g + \Delta\gamma_\psi^t + \Delta\gamma_\psi^f & 1 & -\left(\Delta\alpha_\psi^g + \Delta\alpha_\psi^t + \Delta\alpha_\psi^f\right) & \Delta y_\psi^g + \Delta y_\psi^t + \Delta y_\psi^f \\ -\left(\Delta\beta_\psi^g + \Delta\beta_\psi^t + \Delta\beta_\psi^f\right) & \Delta\alpha_\psi^g + \Delta\alpha_\psi^t + \Delta\alpha_\psi^f & 1 & \Delta z_\psi^g + \Delta z_\psi^t + \Delta z_\psi^f \\ 0 & 0 & 0 & 1 \end{pmatrix} \tag{2}$$

Consider that this machine tool has prefect heat dissipation structure efficiency because each drive motor is designed separately, and so high-speed motorized spindle has the larger influence to the machining accuracy of the machine tool than any other heat source such as the linear guide and the machining during the

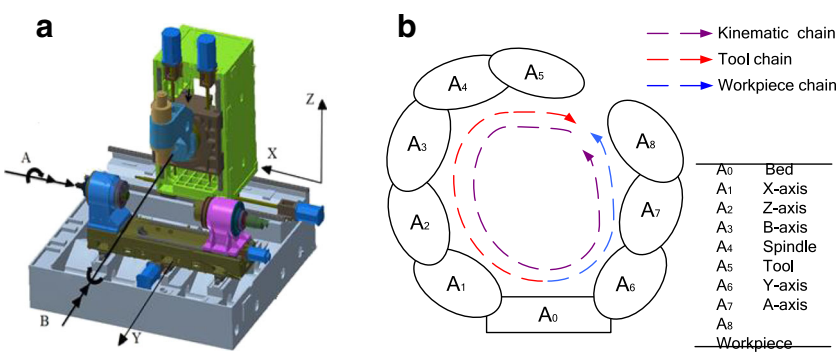

Fig. 1 Three-dimensional model of XKH800 and its coordinate system structure diagram

Table 1 Main parameters of the machine tool

Main parameters of the machine tool	Value
Dimensions of the machine tool	3260 mm*2600 mm*2600 mm
Speed of the spindle	60–10,000 r/min
Journey in the *X*-axis	1250 mm
Journey in the *Y*-axis	400 mm
Journey in the *Z*-axis	400 mm
Range of the *A*-axes	360°
Range of the *B*-axes	±40°
Tool length	180 mm

machining process [50]. Due to the excellent rigidity of the machine tool, the cutting force-induced errors can be neglected. As a result, the thermal-induced errors of the spindle were taken into consideration, together with the geometric errors of the machine and so Eq. (2) can be simplified as

$$\Delta \boldsymbol{K}_{A_3A_4S} = \begin{pmatrix} 1 & -\left(\Delta\gamma_\psi^g + \Delta\gamma_\psi^t\right) & \Delta\beta_\psi^g + \Delta\beta_\psi^t & \Delta x_\psi^g + \Delta x_\psi^t \\ \Delta\gamma_\psi^g + \Delta\gamma_\psi^t & 1 & -\left(\Delta\alpha_\psi^g + \Delta\alpha_\psi^t\right) & \Delta y_\psi^g + \Delta y_\psi^t \\ -\left(\Delta\beta_\psi^g + \Delta\beta_\psi^t\right) & \Delta\alpha_\psi^g + \Delta\alpha_\psi^t & 1 & \Delta z_\psi^g + \Delta z_\psi^t \\ 0 & 0 & 0 & 1 \end{pmatrix} \quad (3)$$

Then, a method of thermal-induced errors modeling based on the fuzzy neural theory is addressed in this paper.

2.1 Comprehensive error modeling

It is supposed that the coordinates of the tool forming point in the tool coordinate system is

$$\mathbf{P}_t = \begin{bmatrix} P_{tx} & P_{ty} & P_{tz} & 1 \end{bmatrix}^{\mathrm{T}} \quad (4)$$

The coordinates of the work-piece forming point in the work-piece coordinate system is

$$\mathbf{P}_w = \begin{bmatrix} P_{wx} & P_{wy} & P_{wz} & 1 \end{bmatrix}^{\mathrm{T}} \quad (5)$$

When the machine tool moves in an ideal form, which means that the machine tool has no errors, the tool forming point and the work-piece forming point will overlap, and so the relationship of $\boldsymbol{K}_{\mathrm{Bed,Tool}}\boldsymbol{P}_t = \boldsymbol{K}_{\mathrm{Bed,Workpiece}}\boldsymbol{P}_{\mathrm{wideal}}$ can be obtained [4] where $\boldsymbol{K}_{\mathrm{Bed,Tool}}$ and $\boldsymbol{K}_{\mathrm{Bed,Workpiece}}$ are the mean homogenous transformation matrix of the tool chain and the homogenous transformation matrix of the workpiece chain, as shown in Fig. 1b, respectively. Then, the terms of $\boldsymbol{K}_{\mathrm{Bed,Tool}} = \left(\prod_{i=0}^{5} \boldsymbol{K}_{\boldsymbol{A_iA_{i+1}}P}\boldsymbol{K}_{\boldsymbol{A_iA_{i+1}}S}\right)\boldsymbol{P}_t$ and $\boldsymbol{K}_{\mathrm{Bed,Workpiece}} = \left(\prod_{i=0,6}^{8} \boldsymbol{K}_{\boldsymbol{A_iA_{i+1}}P}\boldsymbol{K}_{\boldsymbol{A_iA_{i+1}}S}\right)\boldsymbol{P}_w$ are acquired, according to the relationship described in Fig. 1b. Thus, $\boldsymbol{K}_{\mathrm{Bed,Tool}}\boldsymbol{P}_t = \boldsymbol{K}_{\mathrm{Bed,Workpiece}}\boldsymbol{P}_{\mathrm{wideal}}$ can be modified to

$$\left(\prod_{i=0}^{5} \boldsymbol{K}_{\boldsymbol{A_iA_{i+1}}P}\boldsymbol{K}_{\boldsymbol{A_iA_{i+1}}S}\right)\boldsymbol{P}_t = \left(\prod_{i=0,6}^{8} \boldsymbol{K}_{\boldsymbol{A_iA_{i+1}}P}\boldsymbol{K}_{\boldsymbol{A_iA_{i+1}}S}\right)\boldsymbol{P}_w \quad (6)$$

In the present study, the ideal forming function of tool forming point of this five-axis machine tool is

$$\begin{aligned} \boldsymbol{P}_w &= \left(\prod_{i=0,6}^{8} \boldsymbol{K}_{\boldsymbol{A_iA_{i+1}}P}\boldsymbol{K}_{\boldsymbol{A_iA_{i+1}}S}\right)^{-1}\left(\prod_{i=0}^{5} \boldsymbol{K}_{\boldsymbol{A_iA_{i+1}}P}\boldsymbol{K}_{\boldsymbol{A_iA_{i+1}}S}\right)\boldsymbol{P}_t \\ &= \left[\begin{pmatrix}1&0&0&0\\0&1&0&y\\0&0&1&0\\0&0&0&1\end{pmatrix}\begin{pmatrix}1&0&0&0\\0&\cos A&-\sin A&0\\0&\sin A&\cos A&0\\0&0&0&1\end{pmatrix}\begin{pmatrix}1&0&0&x_{wd}\\0&1&0&y_{wd}\\0&0&1&z_{wd}\\0&0&0&1\end{pmatrix}\right]^{-1}\begin{pmatrix}1&0&0&x\\0&1&0&0\\0&0&1&0\\0&0&0&1\end{pmatrix} \\ &\quad\begin{pmatrix}1&0&0&0\\0&1&0&0\\0&0&1&z\\0&0&0&1\end{pmatrix}\begin{pmatrix}\cos B&0&\sin B&0\\0&1&0&0\\-\sin B&0&\cos B&0\\0&0&0&1\end{pmatrix}\begin{pmatrix}\cos\psi&\sin\psi&0&0\\-\sin\psi&\cos\psi&0&0\\0&0&1&0\\0&0&0&1\end{pmatrix}\begin{pmatrix}1&0&0&x_{td}\\0&1&0&y_{td}\\0&0&1&z_{td}\\0&0&0&1\end{pmatrix}\boldsymbol{P}_t \end{aligned} \quad (7)$$

During the actual machining process, the actual position of the cutting tool point will inevitably deviate from the ideal location, which leads to the volumetric error. As a result, the comprehensive volumetric error, induced by the gap between the actual point and ideal point in this paper, can be written as

$$\begin{aligned} E &= \left[\prod_{i=0,6}^{8} \boldsymbol{K}_{\boldsymbol{A_iA_{i+1}}P}\Delta\boldsymbol{K}_{\boldsymbol{A_iA_{i+1}}P}\boldsymbol{K}_{\boldsymbol{A_iA_{i+1}}S}\Delta\boldsymbol{K}_{\boldsymbol{A_iA_{i+1}}S}\right]P_w - \left[\prod_{i=0}^{5} \boldsymbol{K}_{\boldsymbol{A_iA_{i+1}}P}\Delta\boldsymbol{K}_{\boldsymbol{A_iA_{i+1}}P}\boldsymbol{K}_{\boldsymbol{A_iA_{i+1}}S}\Delta\boldsymbol{K}_{\boldsymbol{A_iA_{i+1}}S}\right]p_t \\ &= \boldsymbol{K}_{A_0A_6P}\Delta K_{A_0A_6P}K_{A_0A_6S}\Delta K_{A_0A_6S}K_{A_6A_7P}\Delta K_{A_6A_7P}K_{A_6A_7S}\Delta K_{A_6A_7S}K_{A_7A_8P}\Delta K_{A_7A_8P}K_{A_7A_8S}\Delta K_{A_7A_8S}P_w \\ &\quad -K_{A_0A_1P}\Delta K_{A_0A_1P}K_{A_0A_1S}\Delta K_{A_0A_1S}K_{A_1A_2P}\Delta K_{A_1A_2P}K_{A_1A_2S}\Delta K_{A_1A_2S}K_{A_2A_3P}\Delta K_{A_2A_3P}K_{A_2A_3S}\Delta K_{A_2A_3S} \\ &\quad \cdot K_{A_3A_4P}\Delta K_{A_3A_4P}K_{A_3A_4S}\Delta K_{A_3A_4S}K_{A_4A_5P}\Delta K_{A_4A_5P}K_{A_4A_5S}\Delta K_{A_4A_5S}p_t \end{aligned} \quad (8)$$

Table 2 Characteristic matrices of the five-axis NC machining center

Adjacent body	Body ideal static, motion characteristic matrix $\left(K_{A_iA_{i+1}P}, \boldsymbol{K}_{\boldsymbol{A_iA_{i+1}}S}\right)$	Body static, kinematic error characteristic matrix $\left(\Delta\boldsymbol{K}_{\boldsymbol{A_iA_{i+1}P}}, \Delta\boldsymbol{K}_{\boldsymbol{A_iA_{i+1}}S}\right)$
A_0-A_1	$\boldsymbol{K}_{A_0A_1P} = I_{4\times4}$ $\boldsymbol{K}_{A_0A_1S} = \begin{pmatrix} 1 & 0 & 0 & x \\ 0 & 1 & 0 & 0 \\ 0 & 0 & 1 & 0 \\ 0 & 0 & 0 & 1 \end{pmatrix}$	$\Delta\ \boldsymbol{K}_{A_0A_1P} = I_{4\times4}$ $\Delta\boldsymbol{K}_{A_0A_1S} = \begin{pmatrix} 1 & -\Delta\gamma_x & \Delta\beta_x & \Delta x_x \\ \Delta\gamma_x & 1 & -\Delta\alpha_x & \Delta y_x \\ -\Delta\beta_x & \Delta\alpha_x & 1 & \Delta z_x \\ 0 & 0 & 0 & 1 \end{pmatrix}$
A_1-A_2	$\boldsymbol{K}_{A_1A_2P} = I_{4\times4}$ $\boldsymbol{K}_{A_1A_2\boldsymbol{S}} = \begin{pmatrix} 1 & 0 & 0 & 0 \\ 0 & 1 & 0 & 0 \\ 0 & 0 & 1 & z \\ 0 & 0 & 0 & 1 \end{pmatrix}$	$\Delta\boldsymbol{K}_{A_1A_2P} = \begin{pmatrix} 1 & 0 & \Delta\beta_{xz} & 0 \\ 0 & 1 & -\Delta\alpha_{yz} & 0 \\ -\Delta\beta_{xz} & \Delta\alpha_{yz} & 1 & 0 \\ 0 & 0 & 0 & 1 \end{pmatrix}$ $\Delta K_{A_1A_2S} = \begin{pmatrix} 1 & -\Delta\gamma_z & \Delta\beta_z & \Delta x_z \\ \Delta\gamma_z & 1 & -\Delta\alpha_z & \Delta y_z \\ -\Delta\beta_z & \Delta\alpha_z & 1 & \Delta z_z \\ 0 & 0 & 0 & 1 \end{pmatrix}$
A_2-A_3	$K_{A_2A_3P} = I_{4\times4}$ $K_{A_2A_3S} = \begin{pmatrix} \cos B & 0 & \sin B & 0 \\ 0 & 1 & 0 & 0 \\ -\sin B & 0 & \cos B & 0 \\ 0 & 0 & 0 & 1 \end{pmatrix}$	$\Delta\ K_{A_2A_3P} = \begin{pmatrix} 1 & -\Delta\gamma_{xB} & 0 & 0 \\ \Delta\gamma_{xB} & 1 & -\Delta\alpha_{zB} & 0 \\ 0 & \Delta\alpha_{zB} & 1 & 0 \\ 0 & 0 & 0 & 1 \end{pmatrix}$ $\Delta K_{A_2A_3S} = \begin{pmatrix} 1 & -\Delta\gamma_B & \Delta\beta_B & \Delta x_B \\ \Delta\gamma_B & 1 & -\Delta\alpha_B & \Delta y_B \\ -\Delta\beta_B & \Delta\alpha_B & 1 & \Delta z_B \\ 0 & 0 & 0 & 1 \end{pmatrix}$
A_3-A_4	$K_{A_3A_4P} = I_{4\times4}$ $K_{A_3A_4S} = \begin{pmatrix} \cos\psi & \sin\psi & 0 & 0 \\ -\sin\psi & \cos\psi & 0 & 0 \\ 0 & 0 & 1 & 0 \\ 0 & 0 & 0 & 1 \end{pmatrix}$	$\Delta\ K_{A_3A_4P} = I_{4\times4}$ $\Delta K_{A_3A_4S} = \begin{pmatrix} 1 & -\Delta\gamma_\psi & \Delta\beta_\psi & \Delta x_\psi \\ \Delta\gamma_\psi & 1 & -\Delta\alpha_\psi & \Delta y_\psi \\ -\Delta\beta_\psi & \Delta\alpha_\psi & 1 & \Delta z_\psi \\ 0 & 0 & 0 & 1 \end{pmatrix}$
A_4-A_5	$\boldsymbol{K}_{A_4A_5\boldsymbol{P}} = \begin{pmatrix} 1 & 0 & 0 & x_{td} \\ 0 & 1 & 0 & y_{td} \\ 0 & 0 & 1 & z_{td} \\ 0 & 0 & 0 & 1 \end{pmatrix}$ $\boldsymbol{K}_{A_4A_5S} = I_{4\times4}$	$\Delta\boldsymbol{K}_{A_4A_5\boldsymbol{P}} = \begin{pmatrix} 1 & -\Delta\gamma_{td} & \Delta\beta_{td} & \Delta x_{td} \\ \Delta\gamma_{td} & 1 & -\Delta\alpha_{td} & \Delta y_{td} \\ -\Delta\beta_{td} & \Delta\alpha_{td} & 1 & \Delta z_{td} \\ 0 & 0 & 0 & 1 \end{pmatrix}$ $K_{A_4A_5S} = I_{4\times4}$
A_0-A_6	$\boldsymbol{K}_{A_0A_6P} = I_{4\times4}$ $\boldsymbol{K}_{A_0A_6\boldsymbol{S}} = \begin{pmatrix} 1 & 0 & 0 & 0 \\ 0 & 1 & 0 & y \\ 0 & 0 & 1 & 0 \\ 0 & 0 & 0 & 1 \end{pmatrix}$	$\Delta\ \boldsymbol{K}_{A_0A_6\boldsymbol{P}} = \begin{pmatrix} 1 & -\Delta\gamma_{xy} & 0 & 0 \\ \Delta\gamma_{xy} & 1 & 0 & 0 \\ 0 & 0 & 1 & 0 \\ 0 & 0 & 0 & 1 \end{pmatrix}$ $\Delta\boldsymbol{K}_{A_0A_6\boldsymbol{S}} = \begin{pmatrix} 1 & -\Delta\gamma_y & \Delta\beta_y & \Delta x_y \\ \Delta\gamma_y & 1 & -\Delta\alpha_y & \Delta y_y \\ -\Delta\beta_y & \Delta\alpha_y & 1 & \Delta z_y \\ 0 & 0 & 0 & 1 \end{pmatrix}$
A_6-A_7	$\boldsymbol{K}_{A_6A_7P} = I_{4\times4}$ $\boldsymbol{K}_{A_6A_7\boldsymbol{S}} = \begin{pmatrix} 1 & 0 & 0 & 0 \\ 0 & \cos A & -\sin A & 0 \\ 0 & \sin A & \cos A & 0 \\ 0 & 0 & 0 & 1 \end{pmatrix}$	$\Delta\ \boldsymbol{K}_{A_6A_7\boldsymbol{P}} = \begin{pmatrix} 1 & -\Delta\gamma_{yA} & \Delta\beta_{zA} & 0 \\ \Delta\gamma_{yA} & 1 & 0 & 0 \\ -\Delta\beta_{zA} & 0 & 1 & 0 \\ 0 & 0 & 0 & 1 \end{pmatrix}$ $\Delta\boldsymbol{K}_{A_6A_7\boldsymbol{S}} = \begin{pmatrix} 1 & -\Delta\gamma_a & \Delta\beta_a & \Delta x_a \\ \Delta\gamma_a & 1 & -\Delta\alpha_a & \Delta y_a \\ -\Delta\beta_a & \Delta\alpha_a & 1 & \Delta z_a \\ 0 & 0 & 0 & 1 \end{pmatrix}$
A_7-A_8	$\boldsymbol{K}_{A_7A_8\boldsymbol{P}} = \begin{pmatrix} 1 & 0 & 0 & x_{wd} \\ 0 & 1 & 0 & y_{wd} \\ 0 & 0 & 1 & z_{wd} \\ 0 & 0 & 0 & 1 \end{pmatrix}$ $K_{A_7A_8\boldsymbol{S}} = I_{4\times4}$	$\Delta\boldsymbol{K}_{A_7A_8\boldsymbol{P}} = \begin{pmatrix} 1 & -\Delta\gamma_{wd} & \Delta\beta_{wd} & \Delta x_{wd} \\ \Delta\gamma_{wd} & 1 & -\Delta\alpha_{wd} & \Delta y_{wd} \\ -\Delta\beta_{wd} & \Delta\alpha_{wd} & 1 & \Delta z_{wd} \\ 0 & 0 & 0 & 1 \end{pmatrix}$ $\Delta\ K_{A_7A_8\boldsymbol{S}} = I_{4\times4}$

In the above equation, the values and means of the expressions can be obtained from Table 2.

2.2 Thermal induced errors analysis

The comprehensive error model developed previously includes geometric errors and thermal-induced errors, and these errors should be acquired in order to obtain the comprehensive error model. Among such errors, geometric errors can be obtained by the direct measurement method with measurement tools such as laser interferometer, granite square, and standard mandrel along with sensors. However, thermal-induced errors are more complex, compared to geometric errors, and could not be obtained by the direct measurement method. As a result, a systemic method used for thermal-induced error modeling was proposed based on the fuzzy neural theory to solve this problem, and it contains three parts: temperature measurement point optimization, thermal-induced error analysis of the spindle, and thermal-induced error prediction of the spindle.

In the thermal error modeling of machine tools, where temperature measurement points are clearly an important factor to the accuracy of the thermal error model, the ability to reduce the number of measurement points to simplify the thermal error modeling process while maintaining the desirable modeling accuracy is crucial. There are several strategies for optimization selection of the temperature sensor, such as the principal factor, mutually uncorrelated, and maximum sensitivity. The principal factor which implies that there must be some relevance between each temperature point $T_j(j=1,2,\ldots,m)$ used for thermal error modeling and the thermal error $E_k(k=1,2,\ldots,n)$ is applied to select the temperature measurement points as follows [47]:

$$\chi_j = \frac{\sum_{k=1}^{n}\left(T_{jk}-\overline{T_j}\right)\left(E_k-\overline{E}\right)}{\sqrt{\sum_{k=1}^{n}\left(T_{jk}-\overline{T_j}\right)^2}\sqrt{\sum_{k=1}^{n}\left(E_k-\overline{E}\right)^2}} \tag{9}$$

where $T_j(j=1,2,\ldots,m)$ refers to the temperature set of the j th temperature point; $T_{jk}(j=1,2,\ldots,m;k=1,2,\ldots,n)$ is the k th data of the j th temperature point; E_k is the j th data of the thermal error; $\bar{E}$ and $\overline{T_j}$ refer to the mean value of the thermal error and the j th temperature point, respectively. The temperature points which satisfy $\chi_j > d(|d| \le 1)$ were selected for thermal error modeling.

2.3 Thermal-induced error modeling

The proposed comprehensive error model based on the fuzzy neural theory contains five layers, and its functional structure roughly follows that of reference [15] as presented in Fig. 2.

The first layer is the input layer, and its function is to transfer the inputs. The second layer is the membership function of the inputs, and its main function is to calculate the membership function values of the inputs that are subject to each lingual variable fuzzy set. $\mu_i^j = e^{\frac{(x_i-c_{ij})^2}{\sigma_{ij}}}$ is used as the membership function, where c_{ij} and σ_{ij} are the center and the width of the membership function, respectively. The third layer is the fuzzy rule layer, and each point in this layer stands for a fuzzy rule. Its function is to calculate the fitness value of a corresponding fuzzy rule, as follows: $\alpha_j = \min\{\mu_1^{i_1}, \mu_2^{i_2}, \ldots, \mu_n^{i_n}\}$ *or* $\alpha_j = \mu_1^{i_1}\mu_2^{i_2}\ldots\mu_n^{i_n}$, where $i_1 \in \{1,2,\ldots,m_1\}$; $i_2 \in \{1,2,\ldots,m_2\}$;…; $i_n \in \{1,2,\ldots,m_n\}$. The fourth layer is the fuzzy conclusion layer, and its main function is the normalization of all the fitness values, given as follows: $\overline{\alpha_j} = \frac{\alpha_j}{\sum_{i=1}^{m}\alpha_i}, j = 1,2,\ldots,m.$ The fifth layer is the output layer, and its function is the inverse fuzzy arithmetic: $y_i = \sum_{j=1}^{m}\omega_{ij}\overline{\alpha_j}, i = 1,2,\ldots,r.$

In this way, the function structure of the comprehensive error model based on the fuzzy neural theory has been developed. The next steps include the training of the center of the membership function c_{ij} $(i=1,2,\ldots,r;j=1,2,$

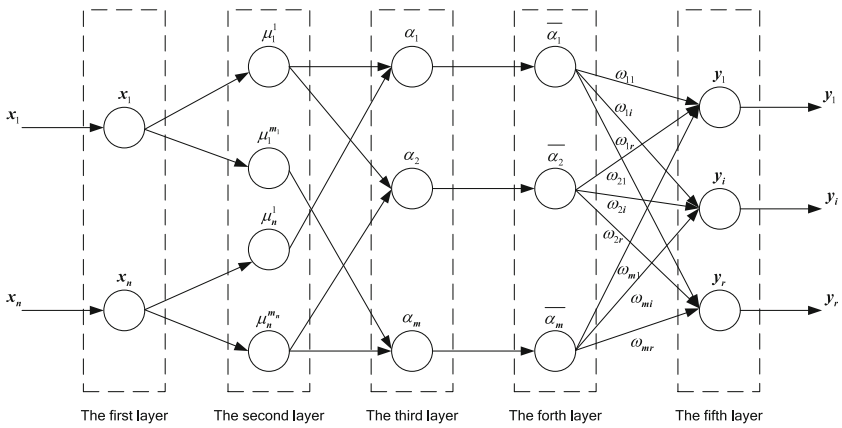

Fig. 2 Thermal error modeling process based on the neural fuzzy control theory

$\ldots, m$), the width of the membership function σ_{ij} in the second layer, and the weight ω_{ij} in the fifth layer. The point functions of each layer can be expressed by the following:

the first layer: $f_i^{(1)} = x_i^{(0)} = x_i, x_i^{(1)} = g_i^{(1)} = f_i^{(1)} (i = 1, 2, \ldots, n)$;

the second layer: $f_{ij}^{(2)} = -\frac{\left(x_i^{(1)} - c_{ij}\right)^2}{\sigma_{ij}^2}$, $x_{ij}^{(2)} = \mu_i^j = g_{ij}^{(2)} = e^{f_{ij}^{(2)}} = e^{-\frac{\left(x_i^{(1)} - c_{ij}\right)^2}{\sigma_{ij}^2}} (i = 1, 2, \ldots, n; j = 1, 2, \ldots, m_i)$;

the third layer: $f_j^{(3)} = \min\left\{x_{1i_1}^{(2)}, x_{2i_2}^{(2)}, \ldots, x_{ni_n}^{(2)}\right\} = \min\left\{\mu_1^{i_1}, \mu_2^{i_2}, \ldots, \mu_n^{i_n}\right\}$ or $f_j^{(3)} = x_{1i_1}^{(2)} x_{2i_2}^{(2)} \ldots x_{ni_n}^{(2)} = \mu_1^{i_1} \mu_2^{i_2} \ldots \mu_n^{i_n}$, $x_j^{(3)} = \alpha_j = g_j^{(3)} = f_j^{(3)} \left(j = 1, 2, \ldots, m; m = \prod_{i=1}^{n} m_i\right)$

the fourth layer: $f_j^{(4)} = \frac{x_j^{(3)}}{\sum_{i=1}^{m} x_i^{(3)}} = \frac{\alpha_j}{\sum_{i=1}^{m} \alpha_i}$, $x_j^{(4)} = \overline{\alpha_j} = g_j^{(4)} = f_j^{(4)} (j = 1, 2, \ldots, m)$;

the fifth layer: $f_i^{(5)} = \sum_{j=1}^{m} \omega_{ij} x_j^{(4)} = \sum_{j=1}^{m} \omega_{ij} \overline{\alpha_j}$ $(i = 1, 2, \ldots, r)$, $x_i^{(5)} = y_i = g_j^{(5)} = f_j^{(5)}$.

Also, the performance index function of this fuzzy neural is given by $E = \frac{1}{2} \sum_{i=1}^{r} (t_i - y_i)^2$, where t_i and y_i refer to the expected output and the actual output, respectively, and then, the first-order gradient algorithm is used for adjusting the parameters ω_{ij}, c_{ij}, σ_{ij}. Their values can be obtained after $k+1$ iterations, as follows:

$$\omega_{ij}(k+1) = \omega_{ij}(k) - \beta \frac{\partial E}{\partial \omega_{ij}} (i = 1, 2, \ldots, r; j = 1, 2, \ldots, m)$$

$$c_{ij}(k+1) = c_{ij}(k) - \beta \frac{\partial E}{\partial c_{ij}} (i = 1, 2, \ldots, n; j = 1, 2, \ldots, m_i)$$

$$\sigma_{ij}(k+1) = \sigma_{ij}(k) - \beta \frac{\partial E}{\partial \sigma_{ij}} (i = 1, 2, \ldots, r; j = 1, 2, \ldots, m)$$

where β is the learning rate and $\vartheta > 0$, E is a set data, while this process ends until $E(k) < E_{\min}$ after the k iterations. As a result, these values of parameters are optimal and can be used for thermal error modeling.

3 Accuracy allocation of NC machine tools

As mentioned above, there are two important issues that have been addressed in this paper: one is to establish a systematic approach to obtain geometric/kinematic errors on the kinematic chain of a machine tool. Another problem, which is considered more important, is to optimize the accuracy allocation of NC machine tools to perform the distribution of the standard deviation for the geometric errors. The first problem has been settled in Section 2. Regarding the second problem, many researchers have focused their attention on the satisfaction of design requirements and the feasibility of processing, neglecting the systemic quantization method for cost and reliability. In this section, the purpose is to propose a general approach, which can be described as the determination of the permissible level of each error source by taking design requirements (machining accuracy) and design specifications (accuracy of each source) as a set of constraints, so that some criteria (in this case, cost and reliability) will be optimized. In order to develop this approach, a geometric error-cost model and a geometric error-reliability model should be established.

3.1 Geometric error-cost modeling

Traditionally, geometric error-cost models were established according to the machining cost of certain components and parts. However, it is difficult to collect the data of the machining cost, and such cost shows significant fluctuations in values among the various manufacturing conditions. Additionally, it is impossible to predict the accurate cost of certain geometric errors. As a result, the fuzzy relatively cost method is used for developing the geometric error-cost model and the solution procedure follows approximately the approach developed in reference [44], although deviates in the formulation used.

According to the weighted function principle [8], it is necessary to consider the influence of errors in various stages of the products to the ultimate accuracy of products. Besides, the difficulty in controlling errors in various stages of the products should not be neglected and it is related to the cost. Therefore, the error which is more difficult to control should be allocated to the larger permitted value and vice versa. Considering the fact that geometric errors come from the relative movements of adjacent bodies, the relative complexity of each geometric errors can be measured by the assembling and adjustment time between these two function components. As a result, the fuzzy assembling cost weight factor of the kth adjacent body, q_k, can be expressed as follows:

$$q_k = \frac{T_k^c}{\sum_{k=1}^{h} T_k^c} \tag{10}$$

where T_k^c refers to the assembling and adjustment time of the kth adjacent body and h is the total number of the whole adjacent bodies.

Then, the weighted average method is used for obtaining the fuzzy assembling cost weight factors of each geometric error. It is supposed that the number of geometric errors of the kth adjacent body is l, containing m linear displacement errors and $l-m$ angular displacement errors. Hence, the fuzzy

assembling cost weight factor of each geometric error can be obtained by:

$$q_i = \begin{cases} \frac{\lambda q_k}{m}, i = 1, 2, \ldots, m \\ \frac{\xi q_k}{l-m}, i = m+1, \ldots, l \end{cases} \quad (11)$$

where λ and ξ are the coefficients of linear displacement errors and angular displacement errors, respectively.

There is a strong relationship between the manufacturing cost of a component and the tolerance specified [4]. The manufacturing cost usually increases with closer tolerances on the quality characteristics as more refined and precise operations are needed and the acceptable range of the output is reduced [38]. However, lesser tolerances usually result into poorer performance, premature wear, and more frequent part rejection. In order to obtain a mathematical expression for the cost-tolerance relationship, many researches have been extensively performed for decades and there are various cost-tolerance models proposed to estimate a proper functional relationship between manufacturing cost and tolerances. In this paper, the exponential curve method was selected to fit the manufacturing data and its typical form for a single feature is formulated as follows [12]:

$$C_M(\Delta_i) = a_i \cdot e^{-b_i \Delta_i} \quad (12)$$

where a_i and b_i are constant coefficients and Δ_i refers to the ith geometric error.

For a machine tool with several geometric errors, the cost can be obtained by

$$C_M(\Delta) = \sum_{i=1}^{n} q_i a_i \cdot e^{-b_i \Delta_i} \quad (13)$$

Quality control is an important function in the manufacturing industry. Inspecting and testing the final products for maintaining high quality while keeping the cost low can allow the manufacturers to stay competitive in the market, which redefine the constraints of traditional quality control [31]. Taguchi and Wu defined a quality loss function (QLF) for measuring quality, and it is a mathematical formula that estimates the loss of quality, resulting from the deviation of the characteristics of a product from their targeted values [39]. There are many types of QLF models, and the quadratic QLF was selected in this paper, as it is considered as a good approximation for measuring the quality of a product, particularly over a range of characteristic values, in the neighborhood of the target values [35]. Due to limited space, a description of the complete analysis was avoided and only the most important results of the quadratic QLF will be presented. Taking q_i into consideration can be modified as

$$L(\Delta) = \psi\left(\frac{1}{16}\sum_{i=1}^{n} q_i(\Delta_i - m_i)\right) = \psi\left(\frac{1}{16}\sum_{i=1}^{n} q_i \Delta_i\right) \quad (14)$$

where Δ_i are the quality characteristics and m_i their target values, in ideal situation $m_i = 0$, while ψ is the quality loss coefficient, which is independent of Δ_i.

Based on the above manufacturing cost and quality loss analysis, the total cost objective function of the machine tool can be formulated as follows:

$$C(\Delta) = q_i[C_M(\Delta) + L(\Delta)] = \sum_{i=1}^{n}\left[q_i a_i \cdot e^{-b_i \Delta_i} + \psi\left(\frac{1}{16}\sum_{i=1}^{n} q_i \Delta_i\right)\right] \quad (15)$$

3.2 Geometric error-reliability modeling

Geometric errors, including pitch errors of the lead screws, straightness errors of the guide ways, angular errors of machine slides, and orthogonal errors among machine axis, are predominately the most important factor of the machine tool machining and assembly process. Although the machining accuracy meets the specifications, while the machine tool is new, it is unable to guarantee that the accuracy is still maintained at the acceptable tolerance range after a long-term operation. The geometric parameter errors are static errors in a short period of time, but after a long period of cutting operations, such errors are dynamically related to factors, such as the errors of the working stage, cutting force-induced errors, tool wear, slide-guideway wear, ambient temperature, or vibration. Consequently, wear will be increased on the interfaces of the various components during machining operations and the accuracy of machine tool will degrade. As a result, the machine tool has to maintain its accuracy for the quality control of the products. In fact, it can be considered as a problem of maintaining and improving the reliability of machine tools by the distribution of geometric errors.

For a general system, reliability can be expressed by the equation of reference [44]:

$$E(G) = \sum_{s \in S} G(s)P(s) \quad (16)$$

where s is the state of a system, S is the state space, $G(s)$ is the reliability evaluation function by taking s as the variable, $P(s)$ denotes the possibility of state s, and $E(G)$ is the expected possibility of $G(s)$.

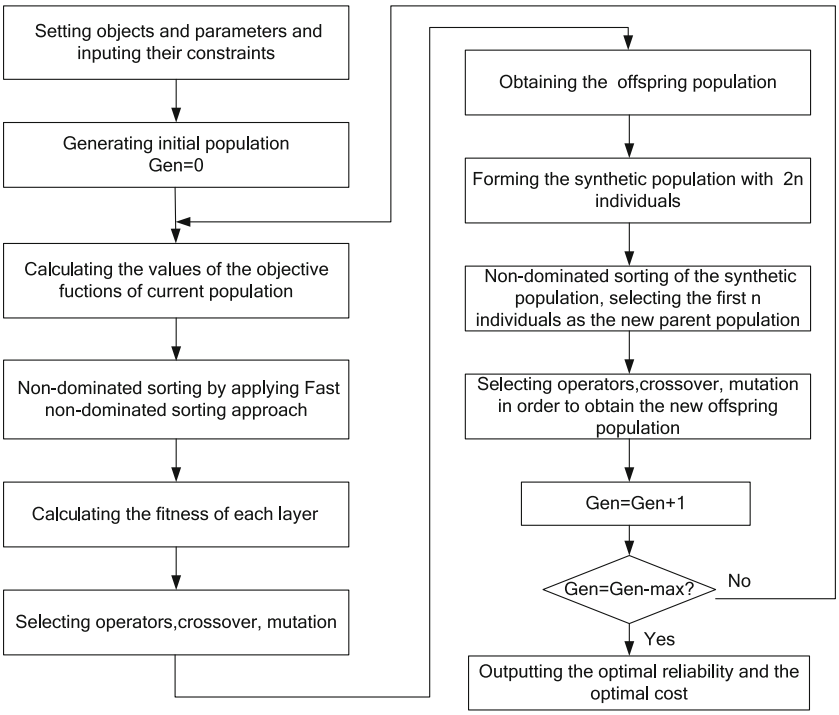

Fig. 3 The algorithm process of the advanced NSGA-II

In this paper, reliability can be expressed as follows:

$$E(\Delta) = \sum_{i=1}^{n} G(\Delta_i) P(\Delta_i) \tag{17}$$

where $G(\Delta_i)$ is the reliability evaluation function, by taking the ith geometric error as the variable, and $P(\Delta_i)$ is the possibility of the ith geometric error promising that the machine tool operates well.

In order to obtain the expression of $P(\Delta_i)$, the frequent failure criterion was applied: the failure of geometric errors, which have the more significant influence on the reliability of the machine tool, should be assigned to the lower reliability and vice versa [34]. In this paper, the possibility of failure of

Table 3 Maximum values of geometric parameter errors of the five-axis NC machine tool

Number i	1	2	3	4	5	6	7	8
Parameter	Δx_x	Δy_x	Δz_x	$\Delta\alpha_x$	$\Delta\beta_x$	$\Delta\gamma_x$	Δx_y	Δy_y
Value	0.0065 mm	0.0065 mm	0.0065 mm	$\left(\frac{0.0037}{1000}\right)^\circ$	$\left(\frac{0.0037}{1000}\right)^\circ$	$\left(\frac{0.0037}{1000}\right)^\circ$	0.007 mm	0.007 mm
Number i	9	10	11	12	13	14	15	16
Parameter	Δz_y	$\Delta\alpha_y$	$\Delta\beta_y$	$\Delta\gamma_y$	Δx_z	Δy_z	Δz_z	$\Delta\alpha_z$
Value	0.007 mm	$\left(\frac{0.0028}{1000}\right)^\circ$	$\left(\frac{0.0028}{1000}\right)^\circ$	$\left(\frac{0.0028}{1000}\right)^\circ$	0.007 mm	0.007 mm	0.007 mm	$\left(\frac{0.0028}{1000}\right)^\circ$
Number i	17	18	19	20	21	22	23	24
Parameter	$\Delta\beta_z$	$\Delta\gamma_z$	Δx_φ	Δy_φ	Δz_φ	$\Delta\alpha_\varphi$	$\Delta\beta_\varphi$	$\Delta\gamma_\varphi$
Value	$\left(\frac{0.0028}{1000}\right)^\circ$	$\left(\frac{0.0028}{1000}\right)^\circ$	0.0058 mm	0.0058 mm	0.0058 mm	$\left(\frac{0.0061}{1000}\right)^\circ$	$\left(\frac{0.0061}{1000}\right)^\circ$	$\left(\frac{0.0061}{1000}\right)^\circ$
Number i	25	26	27	28	29	30	31	32
Parameter	Δx_A	$\Delta\gamma_A$	Δz_A	$\Delta\alpha_A$	$\Delta\beta_A$	$\Delta\gamma_A$	Δx_B	Δy_B
Value	0.0058 mm	0.0058 mm	0.0058 mm	$\left(\frac{0.0061}{1000}\right)^\circ$	$\left(\frac{0.0061}{1000}\right)^\circ$	$\left(\frac{0.0061}{1000}\right)^\circ$	0.0068 mm	0.0068 mm
Number i	33	34	35	36	37	38	39	40
Parameter	Δz_B	$\Delta\alpha_B$	$\Delta\beta_B$	$\Delta\gamma_B$	$\Delta\gamma_{xy}$	$\Delta\beta_{xz}$	$\Delta\alpha_{yz}$	$\Delta\gamma_{yA}$
Value	0.0068 mm	$\left(\frac{0.0049}{1000}\right)^\circ$	$\left(\frac{0.0049}{1000}\right)^\circ$	$\left(\frac{0.0049}{1000}\right)^\circ$	$\left(\frac{0.0037}{500}\right)^\circ$	$\left(\frac{0.0037}{500}\right)^\circ$	$\left(\frac{0.0037}{500}\right)^\circ$	$\left(\frac{0.011}{300}\right)^\circ$
Number i	41	42	43					
Parameter	$\Delta\beta_{zA}$	$\Delta\gamma_{xB}$	$\Delta\alpha_{zB}$					
Value	$\left(\frac{0.011}{300}\right)^\circ$	$\left(\frac{0.011}{300}\right)^\circ$	$\left(\frac{0.011}{300}\right)^\circ$					

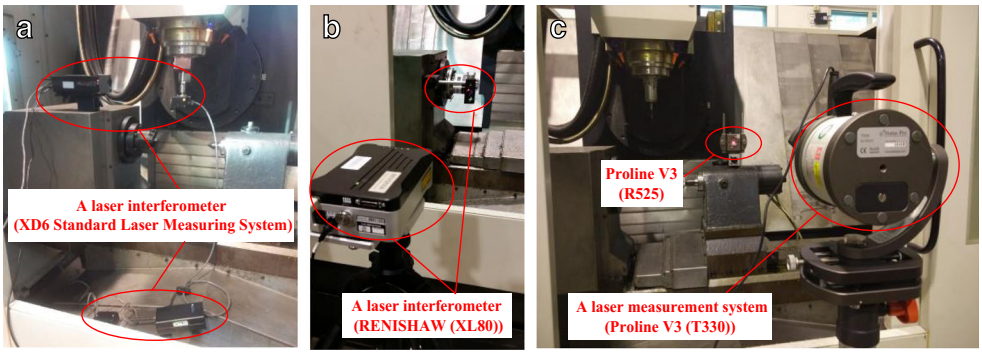

Fig. 4 Geometric error measurement methods. **a** The measurement method of the prismatic joint errors. **b** The measurement method of the rotary joint errors. **c** The measurement method of the squareness errors and the parallelism errors

geometric errors can be obtained by the possibility of failure of components, which can be calculated as follows:

$$\alpha_j = 1 - \frac{T_j^a}{T_j^t} \tag{18}$$

where T_j^t refers to the ideal working time and T_j^a refers to the actual working time.

Hence, the possibility of failure of geometric errors can be obtained by:

$$\beta_i = \frac{\alpha_j + \alpha_k}{2} \tag{19}$$

where α_j and α_k are the possibilities of failure of these two adjacent components, respectively, whose relative motion generates the geometric error Δ_i.

As a result, the possibility of the machine tool operating well can be expressed by

$$P(\Delta_i) = 1 - \beta_i \tag{20}$$

To date, the possibility of the machine tool operating well $P(\Delta_i)$ has been obtained. In order to acquire the reliability of the machine tool, the reliability evaluation function $G(\Delta_i)$ should be studied. Failure criticality is another criterion used for evaluating the reliability of

Table 4 Initial values of geometric parameter errors of the five-axis NC machine tool

Number i	1	2	3	4	5	6	7	8
Parameter	Δx_x	Δy_x	Δz_x	$\Delta\alpha_x$	$\Delta\beta_x$	$\Delta\gamma_x$	Δx_y	Δy_y
Value	0.0061 mm	0.0061 mm	0.0061 mm	$\left(\frac{0.0032}{1000}\right)^\circ$	$\left(\frac{0.0032}{1000}\right)^\circ$	$\left(\frac{0.0032}{1000}\right)^\circ$	0.0063 mm	0.0063 mm
Number i	9	10	11	12	13	14	15	16
Parameter	Δz_y	$\Delta\alpha_y$	$\Delta\beta_y$	$\Delta\gamma_y$	Δx_z	Δy_z	Δz_z	$\Delta\alpha_z$
Value	0.0063 mm	$\left(\frac{0.0025}{1000}\right)^\circ$	$\left(\frac{0.0025}{1000}\right)^\circ$	$\left(\frac{0.0025}{1000}\right)^\circ$	0.0064 mm	0.0064 mm	0.0064 mm	$\left(\frac{0.0026}{1000}\right)^\circ$
Number i	17	18	19	20	21	22	23	24
Parameter	$\Delta\beta_z$	$\Delta\gamma_z$	Δx_φ	Δy_φ	Δz_φ	$\Delta\alpha_\varphi$	$\Delta\beta_\varphi$	$\Delta\gamma_\varphi$
Value	$\left(\frac{0.0026}{1000}\right)^\circ$	$\left(\frac{0.0026}{1000}\right)^\circ$	0.0051 mm	0.0051 mm	0.0051 mm	$\left(\frac{0.0056}{1000}\right)^\circ$	$\left(\frac{0.0056}{1000}\right)^\circ$	$\left(\frac{0.0056}{1000}\right)^\circ$
Number i	25	26	27	28	29	30	31	32
Parameter	Δx_A	Δy_A	Δz_A	$\Delta\alpha_A$	$\Delta\beta_A$	$\Delta\gamma_A$	Δx_B	Δy_B
Value	0.0054 mm	0.0054 mm	0.0054 mm	$\left(\frac{0.0056}{1000}\right)^\circ$	$\left(\frac{0.0056}{1000}\right)^\circ$	$\left(\frac{0.0056}{1000}\right)^\circ$	0.0062 mm	0.0062 mm
Number i	33	34	35	36	37	38	39	40
Parameter	Δz_B	$\Delta\alpha_B$	$\Delta\beta_B$	$\Delta\gamma_B$	$\Delta\gamma_{xy}$	$\Delta\beta_{xz}$	$\Delta\alpha_{yz}$	$\Delta\gamma_{yA}$
Value	0.0062 mm	$\left(\frac{0.0048}{1000}\right)^\circ$	$\left(\frac{0.0048}{1000}\right)^\circ$	$\left(\frac{0.0048}{1000}\right)^\circ$	$\left(\frac{0.0032}{500}\right)^\circ$	$\left(\frac{0.0032}{500}\right)^\circ$	$\left(\frac{0.0032}{500}\right)^\circ$	$\left(\frac{0.007}{300}\right)^\circ$
Number i	41	42	43					
Parameter	$\Delta\beta_{zA}$	$\Delta\gamma_{xB}$	$\Delta\alpha_{zB}$					
Value	$\left(\frac{0.008}{300}\right)^\circ$	$\left(\frac{0.008}{300}\right)^\circ$	$\left(\frac{0.008}{300}\right)^\circ$					

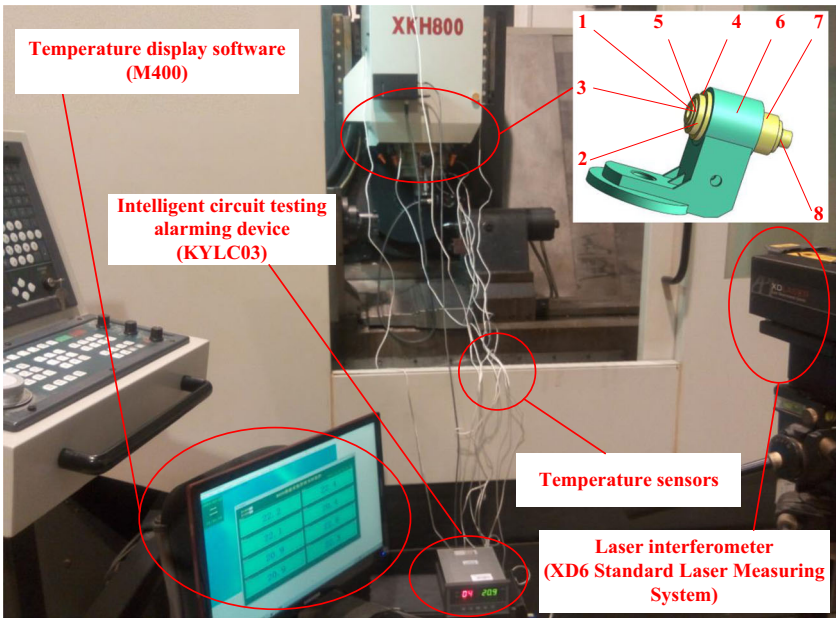

Fig. 5 Measuring the temperatures of temperature measurement points and the thermal errors of the *X*-axis, *Y*-axis, and *Z*-axis

machine tools and can be expressed by the maintenance and adjustment time after failure occurs. Hence, the possibility of fallback of certain component can be given by

$$\varepsilon_k = \frac{T_k^f}{\sum_{k=1}^{h} T_k^f} \tag{21}$$

Hence, the weight factor of fallback of geometric error is expressed as follows:

$$\mu_i = \frac{\varepsilon_j + \varepsilon_k}{2} \tag{22}$$

In view that there is a negative correlation between geometric errors and the operating state of machine tools, the reliability evaluation function is obtained by

$$G(\Delta_i) = \frac{\eta_i \mu_i}{\Delta_i} \tag{23}$$

where η_i is the coefficient of reliability. As a result, the geometric error-reliability model can be acquired by

$$R(\Delta_i) = E(\Delta_i) = \sum_{i=1}^{n} \frac{\eta_i \mu_i}{\Delta_i}(1-\beta_i) \tag{24}$$

3.3 Proposed accuracy allocation approach

Up to date, the allocation and optimization problem has been formulated to minimize the cost and maximize the reliability

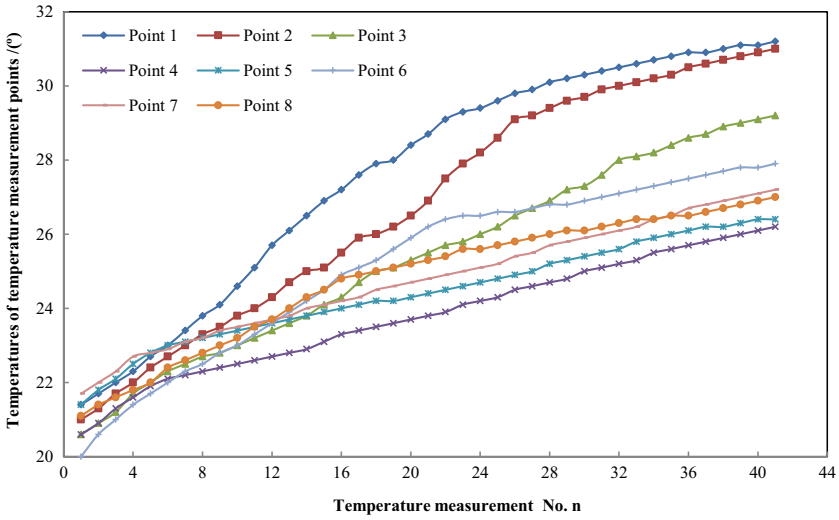

Fig. 6 Temperatures of eight temperature measurement points

subject to the geometric and operational constraints. Hence, the accuracy allocation of the multi-axis machine tool is described as a two-objective optimization problem. The optimization model can be represented as follows:

$$\begin{cases} M_1(\text{minimize}) = \min[C_M(\Delta) + L(\Delta)] = \min\sum_{i=1}^{n} q_i \left[a_i \cdot e^{-b_i \Delta_i} + \psi\left(\frac{1}{16}\sum_{i=1}^{n} \Delta_i\right)\right] \\ M_2(\text{maximize}) = \max R(\Delta) = \max\left[\sum_{i=1}^{n} \frac{\eta_i \mu_i}{\Delta_i}(1-\beta_i)\right] \end{cases} \quad (25)$$

subject to

$$\begin{cases} \sum_{i=1}^{n} q_i = 1 \\ \sum_{i=1}^{n} \mu_i = 1 \\ \beta_i \le 3\% \\ \max(E_x) \le def(E_x) \\ \max(E_y) \le def(E_y) \\ \max(E_z) \le def(E_z) \\ \Delta_i \in \Delta \\ 0 \le \Delta_i \le def(\Delta_i) \quad (i = 1, 2, \ldots, n) \end{cases}$$

In the preceding section, an accuracy allocation model of this machine tool has been established and the process of optimization was conducted by the MatLab software. In this paper, the advanced NSGA-II is introduced as the optimization algorithm [44] for obtaining the optimal cost and reliability and its algorithm process is presented in Fig. 3.

4 Application and verification

The work performed in this study is presented as a procedure for finding the tolerance specifications on the parameters of geometric errors in order to perform the accuracy allocation of the multi-axis machine tool.

According to "Test code for machine tools—part 1: geometric accuracy of machines operating under no-load

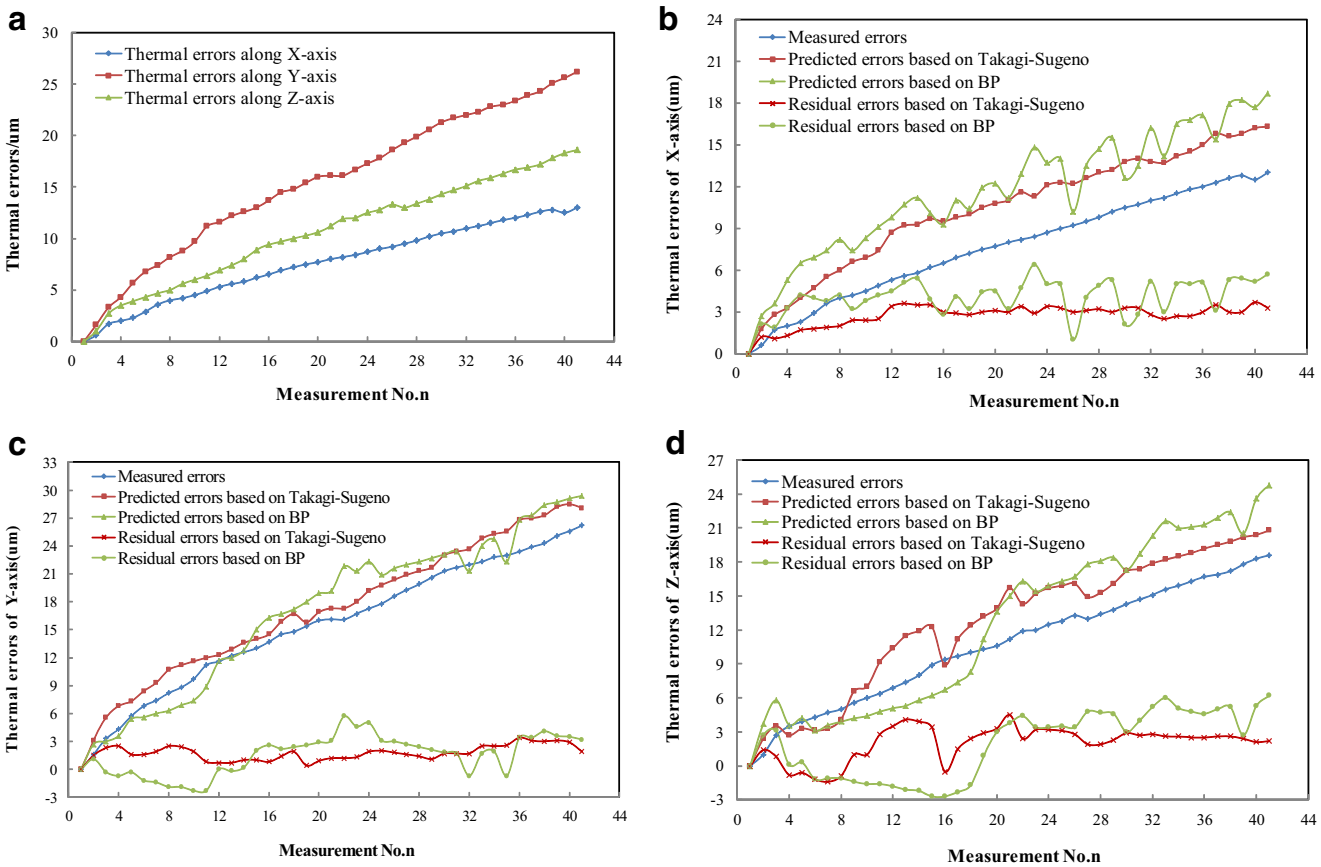

Fig. 7 Results of the thermal error experiment. **a** Measured thermal errors of the *X*-axis, *Y*-axis, and *Z*-axis. **b** Thermal errors of the *X*-axis. **c** Thermal errors of the *Y*-axis. **d** Thermal errors of the *Z*-axis

Table 5 Performance comparison of two network models (unit:μm)

	Network type	Maximum absolute deviation	Mean square error
X-axis	Residual errors (BP)	6.4	1.333563
	Residual errors (Takagi-Sugeno)	3.7	0.794278
Y-axis	Residual errors (BP)	5.7	2.115131
	Residual errors (Takagi-Sugeno)	3.1	0.798115
Z-axis	Residual errors (BP)	6.2	2.954661
	Residual errors (Takagi-Sugeno)	4.5	1.499801

or finishing conditions" and "Test code for machine tools—part 2: determination of accuracy and repeatability of positioning numerically controlled axes," the values of geometric parameter errors of the five-axis NC machine tool were set as the constraints and are presented in Table 3.

In order to perform the comprehensive error modeling, geometric errors can be initially measured firstly and different

Table 6 Values of the fuzzy cost weight factor, the weight factor of fallback, and the possibility of failure

Error number	Fuzzy cost weight factor q_i	Weight factor of fallback μ_i	Possibility of failure β_i
1	0.026	0.025	0.031
2	0.026	0.025	0.031
3	0.026	0.025	0.031
4	0.024	0.025	0.031
5	0.024	0.025	0.031
6	0.024	0.025	0.031
7	0.024	0.022	0.028
8	0.024	0.022	0.028
9	0.024	0.022	0.028
10	0.023	0.022	0.028
11	0.023	0.022	0.028
12	0.023	0.022	0.028
13	0.023	0.021	0.029
14	0.023	0.021	0.029
15	0.023	0.021	0.029
16	0.021	0.021	0.029
17	0.021	0.021	0.029
18	0.021	0.021	0.029
19	0.028	0.027	0.037
20	0.028	0.027	0.037
21	0.028	0.027	0.037
22	0.023	0.027	0.037
23	0.023	0.027	0.037
24	0.023	0.027	0.037
25	0.019	0.024	0.026
26	0.019	0.024	0.026
27	0.019	0.024	0.026
28	0.024	0.024	0.026
29	0.024	0.024	0.026
30	0.024	0.024	0.026
31	0.02	0.023	0.025
32	0.02	0.023	0.025
33	0.02	0.023	0.025
34	0.023	0.023	0.025
35	0.023	0.023	0.025
36	0.023	0.023	0.025
37	0.024	0.02	0.023
38	0.024	0.02	0.023
39	0.024	0.02	0.023
40	0.023	0.022	0.027
41	0.023	0.022	0.027
42	0.024	0.022	0.027
43	0.024	0.022	0.027

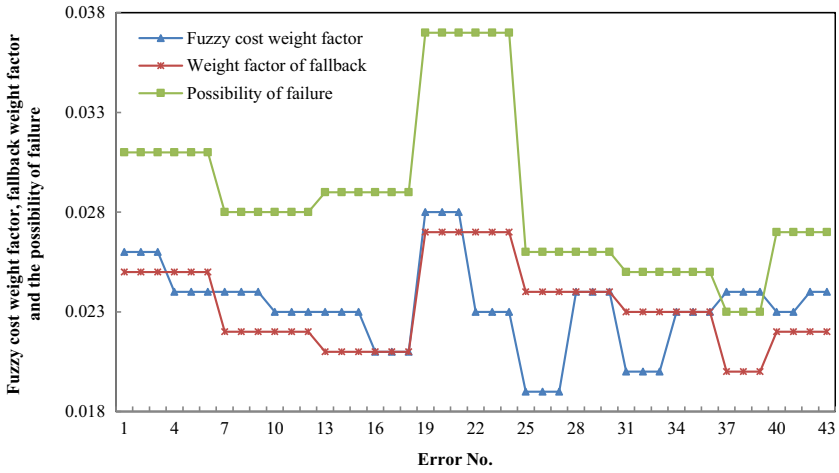

Fig. 8 Fuzzy cost weight factor, fallback weight factor, and the possibility of failure

geometric parameter errors have different methods in the measurement process, as follows:

1) The prismatic joint errors are *X*-prismatic errors (error no.1–no.6 in Table 3), *Y*-prismatic errors (error no.7–no.12 in Table 3), and *Z*-prismatic errors (error no.13–no.18 in Table 3), and a laser interferometer (XD6 Standard Laser Measuring System) was used to measure them, as presented in Fig. 4a. The rotary joint errors are *A*-prismatic errors (error no.19–no.24 in Table 3), *B*-prismatic errors (error no.25–no.30 in Table 3), and the spindle errors (error no.31–no.36 in Table 3), and another laser interferometer (RENISHAW (XL80)) and a mirror were used to measure them, as presented in Fig. 4b.

2) A laser measurement system (Proline V3) was utilized to quantify the squareness errors of prismatic joints (error no.37–no.39) and the parallelism errors of rotary joints, including the parallelism errors for *A*-joint and *B*-joint errors of the *A*-axis and *B*-axis (error no.40–no.43), as presented in Fig. 4c. A laser transmitter (T330) was used to transmit the laser, and a laser receiver (R525), placed on another axis, was used to receive the laser transmitted by T330. Then, the squareness errors of the prismatic joints and the parallelism errors of the rotary joint can be measured, respectively, by such laser.

According to the above measurement methods, the initial values of geometric parameter errors were obtained and are presented in Table 4. Compared to the measurement of geometric errors, thermal-induced error prediction is considered as the more important aspect in this paper.

The experimental conditions of the thermal-induced error prediction can be described as follows: the spindle of the five-axis NC machine tool (XKH800) runs for a certain time at the typical speed with no load, which makes it unnecessary to equip the tool and the workpiece [50]. As a result, there is no machining process and, thus, the only parameter that can be considered is the speed of the spindle. Also, an intelligent circuit testing alarming device (KYLC03) was used to measure the temperatures and a laser interferometer (XD6 Standard Laser Measuring System) was used to measure the thermal errors of the *X*-axis, *Y*-axis, and *Z*-axis.

The experiment was designed as follows: eight temperature measurement points (point 1 to point 8), which had the larger correlation with thermal errors, were arranged according to the preliminary analysis of the structure and the working conditions of this machine tool, and the measurement process, including the installation of the location, is presented in Fig. 5. During the experiment, the spindle of this machine tool runs for 160 min at the speed of 2000 rpm, with no load. The intelligent circuit testing alarming device (KYLC03) was used to simultaneously measure the temperature of these eight points, and the laser interferometer (XD6 Standard Laser Measuring System) was used to measure the thermal errors of the *X*-axis, *Y*-axis, and *Z*-axis, with a sampling repetition of 4 min. The total number of measurement was 41, and then, the first group of thermal error measurement data used as the modeling sample was obtained. After the machine tool was cooled down, the second group of thermal error measurement

Table 7 Part results of the NSGA-II optimization algorithms

Optimization objects	Initial value	Optimization results				
		No.1	No.2	No.3	No.4	No.5
$C(\Delta)$	8.12 E4	9.27 E4	11.96 E4	18.78 E4	29.65 E4	5.88 E05
$R(\Delta)$	313.76	316.56	317.33	318.20	322.65	324.86

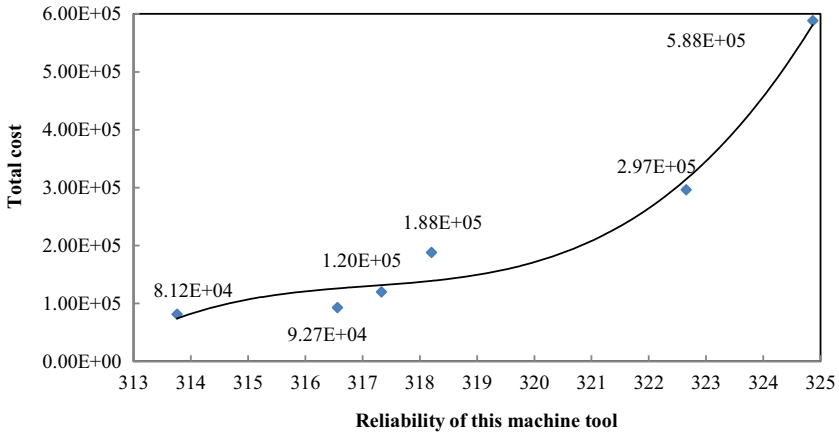

Fig. 9 The relationship between the total cost and the reliability of this machine tool

data used to check the predictive ability of the model developed was obtained by the same way.

According to the thermal error measurement data collected, the temperature values of the eight temperature measurement points are presented in Fig. 6 and the results of thermal errors of the *X*-axis, *Y*-axis, and *Z*-axis are presented in Fig. 7a. Too many temperature measurement points will increase the complexity of thermal error modeling, which will affect the modeling efficiency, and as a result, a temperature measurement point optimization technique, called principal factor, was applied in this paper and the four temperature measurement points (point 1, point 2, point 4, and point 8), which presented the largest correlation with the thermal errors, were obtained.

In order to develop the thermal error model, the temperature of these four points was used as the input parameters and the thermal errors were used as the output parameters. The fuzzy set of every input parameter contains three fuzzy subsets, which means that there are 3^4 fuzzy rules in total, and then, the thermal error model, based on Takagi-Sugeno introduced in the preceding sections, was programmed in the MatLab software. For verification and comparison of the proposed model, the second group of the four temperature measurement points was added to this model as the input parameters to predict the thermal errors. The predicted values and the measured values of thermal errors were compared to verify the thermal error model, based on Takagi-Sugeno. Furthermore, a common method of error modeling, called BP neural network, was used to verify the effectiveness of this model. In the BP network, the number of hidden layer units is generally defined by the formula $s = \sqrt{m+n} + a$ (where m, n is the number of input and output units, $a \in [1, 10]$). The comparison of the predicted value and the measured value of thermal errors of the *X*-axis, *Y*-axis, and *Z*-axis is presented in Fig. 7b–d. From Fig. 7b–d, it is clear that the residual errors between the predicted value and the measured value are relatively small, which implies that the model proposed in this paper has very good prediction ability. The residual errors of the model based on Takagi-Sugeno and the model based on BP respectively compared with each other are also presented in Fig. 7. Table 5 is drawn from Fig. 7, and it can be observed that the residual error of Takagi-Sugeno is significantly smaller than that of the BP neural network, which means that the model based on Takagi-Sugeno has better prediction ability.

In light of the accumulated large design experience and test information of the enterprise for a long time, the fuzzy cost weight factor q_i, the weight factor of fallback μ_i, and the possibility of failure β_i, of each geometric error, can be acquired as presented in Table 6. Figure 8 shows the weight factors of the fuzzy cost, fallback, and the possibility of failure, as drawn from Table 6. From Fig. 8, it can be observed that different errors have different influence impact on the fuzzy cost, fallback, and the possibility of failure. Also, $\boldsymbol{a}_i = 1$; $\psi = 1$; $\boldsymbol{b}_i = 1$, $\eta_i = 1$ as to linear displacement error, and $\boldsymbol{b}_i = 8.0e^{-4}$, $\eta_i = 5.0e^{-2}$ as to

Table 8 Comparison of various optimization algorithms

Evaluation objects	Initial value	Results of NSGA	Results of NSGA-II
Time of algorithm	–	510.26	380.68
Number of individuals	–	28.5 %	37.2 %
$C(\Delta)$	8.12 E4	9.64 E4	9.27 E4
$R(\Delta)$	313.76	316.24	316.56

Table 9 Optimal values of geometric parameter errors of the five-axis NC machine tool

Number i	1	2	3	4	5	6	7	8
Parameter	Δx_x	Δy_x	Δz_x	$\Delta\alpha_x$	$\Delta\beta_x$	$\Delta\gamma_x$	Δx_y	Δy_y
Value	0.0055 mm	0.0055 mm	0.0055 mm	$\left(\frac{0.0028}{1000}\right)^\circ$	$\left(\frac{0.0028}{1000}\right)^\circ$	$\left(\frac{0.0028}{1000}\right)^\circ$	0.0056 mm	0.0056 mm
Number i	9	10	11	12	13	14	15	16
Parameter	Δz_y	$\Delta\alpha_y$	$\Delta\beta_y$	$\Delta\gamma_y$	Δx_z	Δy_z	Δz_z	$\Delta\alpha_z$
Value	0.0056 mm	$\left(\frac{0.0025}{1000}\right)^\circ$	$\left(\frac{0.0025}{1000}\right)^\circ$	$\left(\frac{0.0025}{1000}\right)^\circ$	0.0056 mm	0.0056 mm	0.0056 mm	$\left(\frac{0.0023}{1000}\right)^\circ$
Number i	17	18	19	20	21	22	23	24
Parameter	$\Delta\beta_z$	$\Delta\gamma_z$	Δx_φ	Δy_φ	Δz_φ	$\Delta\alpha_\varphi$	$\Delta\beta_\varphi$	$\Delta\gamma_\varphi$
Value	$\left(\frac{0.0023}{1000}\right)^\circ$	$\left(\frac{0.0023}{1000}\right)^\circ$	0.0047 mm	0.0047 mm	0.0047 mm	$\left(\frac{0.0051}{1000}\right)^\circ$	$\left(\frac{0.0051}{1000}\right)^\circ$	$\left(\frac{0.0051}{1000}\right)^\circ$
Number i	25	26	27	28	29	30	31	32
Parameter	Δx_A	Δy_A	Δz_A	$\Delta\alpha_A$	$\Delta\beta_A$	$\Delta\gamma_A$	Δx_B	Δy_B
Value	0.005 mm	0.005 mm	0.005 mm	$\left(\frac{0.0054}{1000}\right)^\circ$	$\left(\frac{0.0054}{1000}\right)^\circ$	$\left(\frac{0.0054}{1000}\right)^\circ$	0.0055 mm	0.0055 mm
Number i	33	34	35	36	37	38	39	40
Parameter	Δz_B	$\Delta\alpha_B$	$\Delta\beta_B$	$\Delta\gamma_B$	$\Delta\gamma_{xy}$	$\Delta\beta_{xz}$	$\Delta\alpha_{yz}$	$\Delta\gamma_{yA}$
Value	0.0055 mm	$\left(\frac{0.0048}{1000}\right)^\circ$	$\left(\frac{0.0048}{1000}\right)^\circ$	$\left(\frac{0.0048}{1000}\right)^\circ$	$\left(\frac{0.003}{500}\right)^\circ$	$\left(\frac{0.003}{500}\right)^\circ$	$\left(\frac{0.003}{500}\right)^\circ$	$\left(\frac{0.0062}{300}\right)^\circ$
Number i	41	42	43					
Parameter	$\Delta\beta_{zA}$	$\Delta\gamma_{xB}$	$\Delta\alpha_{zB}$					
Value	$\left(\frac{0.0062}{300}\right)^\circ$	$\left(\frac{0.0062}{300}\right)^\circ$	$\left(\frac{0.0062}{300}\right)^\circ$					

angular displacement error. In the algorithm process of the advanced NSGA-II, it is supposed that $N=200$, Gen-max = 20, the possibility of crossover is 0.8, and the possibility of mutation is 0.5. Then, the results of the optimization model (Eq. (25)) by applying the NSGA-II optimization algorithm were obtained, which were a set of points. In order to acquire to the optimal reliability and cost, five points (no.1–no.5), which cover the range of the results of the reliability, were selected from the optimization results, as presented in Table 7. Figure 9 is drawn according to Table 7, demonstrating the relationship between the total cost and the reliability of this machine tool, using the total cost and the reliability as the ordinate and the abscissa, respectively. For each value of the reliability of such five optimization points selected from Table 7, the values of the corresponding cost were presented as the ordinate of the optimization points in Fig. 9. From Fig. 9, it can be derived that when the reliability improvement is not too tight, it seems that the cost shows a moderate increase. However, as the reliability tightens, the cost tends to rise straightly. As a result, there is no need to design the machine tool with the highest reliability and so, the final process of design optimization of the multi-axis NC machine tool is point 1, whose reliability satisfies the design requirements while total cost is optimal at the same time.

In order to verify the advanced NSGA-II is superior, the NSGA was used for comparison and the optimization results can be obtained in Table 8. From Table 8, it can be observed that the time of algorithm of the advanced NSGA-II is less than that of NSGA and the number of individuals is more than that of NSGA. As a result, NSGA-II can be considered as more suitable for applying into solving such two-objective optimization problem. According to the optimization results of the reliability and the cost, the optimal values of geometric parameter errors of five-axis NC machine tool were obtained as shown in Table 9.

In order to verify the effectiveness of the optimization results according to NSGA-II, experiments were performed on a five-axis machining center (XKH800), which can process various materials and shapes. Such machining center has

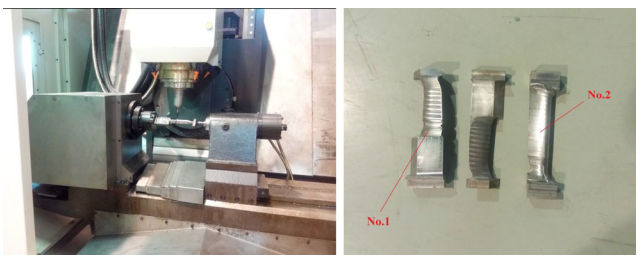

Fig. 10 The five-axis machining center (XKH800) and workpieces of various types used for machining

Table 10 The material of the blades and the machining parameters of the experiments

blades	Material	Machining tool	Tool	Cutting depth/ (mm)	Speed of the spindle/ (r/min)	Feed engagement/ (mm/z)	Feed row-with/ (mm)
No.1	45#	XKH800	High-speed steel ball end milling cutter	0.5	2000	0.1	0.2
No.2				1	2000	0.15	0.3

processed three blades of two different types everyday continuously for 40 weeks, including three distinct periods: no.1–10 weeks (before optimization), no.11–20 weeks (after optimization), and no.20–30 weeks (after optimization). The five-axis machining center (XKH800) and its workpieces are presented in Fig. 10, and the material of the blades and the machining parameters are given in Table 10. During the experiments, the failure number was recorded to calculate the possibility of failure of this machine tool and the test results are presented in Table 11. From Table 11, it can be observed that before optimization, the possibility of failure of this machine tool was higher than 3 %, which failed to meet the basic design requirements of this machine tool, but after optimization of the geometric parameter errors, the possibility of failure of this machine tool was less than 3 %, meeting the design requirements of this machine tool and implying that the reliability of this machine tool has been improved. However, it is also clear that there was a slight increase of the possibility of failure from no.21 weeks to no.30 weeks, which was contributed to the degradation of geometric parameter errors. As a result, the geometric parameter errors after optimization satisfied the design requirements of this machine tool in a long period of time, implying that the reliability of this machine tool has been improved. Hence, the proposed approach in this paper was verified.

5 Conclusions

In this paper, we simultaneously consider geometric errors and thermal-induced errors and have addressed the cost-accuracy trade-off problem associated with the multi-axis NC machine tools. The approach proposed in this study is focused around developing a general methodology for optimizing the total cost (manufacture and QLF) and reliability of multi-axis machine tools, and it is a process of reallocating of each geometric error. This was performed by taking the minimum cost and maximum reliability of machine tools as criteria and taking the machining accuracy of machine tools as constraint, to optimize the basic geometric parameter errors of machine tools. This study contains the following:

(1) A comprehensive volumetric error model, showing the coupling relationship between the individual errors of the components of this machine tool and its volumetric accuracy, was established by applying the multi-body system (MBS) theory. Also, the thermal error model based on the neural fuzzy control theory was developed and compared to the BP neural network.
(2) Based on the traditional manufacturing cost model, the quality loss analysis model, and the reliability analysis model of a system, a geometric error-cost model and a geometric error-reliability model were developed, taking the weighted function principle into consideration.
(3) An approach that simultaneously considers cost and reliability to allocate geometric accuracy of components for improving machining accuracy reliability was proposed. Such approach has been formulated into a mathematical model to minimize the cost and maximize the reliability subject to the geometric and operational constraints.
(4) Based on the previous theoretical research, a demonstration was performed in a five-axis machine tool that was used to verify this approach. The advanced NSGA-II was introduced as the optimized algorithm, and the cost and reliability were optimized.

In terms of the shortcomings of the work and areas for future studies, the following issues would be suggested for further investigation: this work considers only the geometric

Table 11 Results of the reliability of this machine tool in each period

Periods	Blades	Test number	Number of failure	Possibility of failure (%)
No.1–10 weeks	No.1	210	10	4.76
(before optimization)	No.2	210	11	5.24
No.11–20 weeks	No.1	210	5	2.38
(after optimization)	No.2	210	4	1.90
No.21–30 weeks	No.1	210	6	2.86
(after optimization)	No.2	210	5	2.38

errors and thermal-induced errors. In fact, the load errors induced by the joint interface deformation between the structural components of the machine tool also contribute to the volumetric machining accuracy. As a result, the extension to the load errors should be considered in future research.

Acknowledgments The authors are most grateful to the National Natural Science Foundation of China (51575009) and the Jing-Hua Talents Project of Beijing University of Technology, the National Science and Technology Major Project (2014ZX04010-011), the National Natural Science Foundation of China (No. 51575010), Beijing Nova Program (Z1511000003150138), the Leading Talent Project of Guangdong Province, Open Project of the State Key Lab of Digital Manufacturing Equipment and Technology (Huazhong University of Science and Technology), Shantou Light Industry Equipment Research Institute of Science and Technology Correspondent Station (2013B090900008), and the National Science and Technology Major Project (2013ZX04013-011) for supporting the research work that was presented in this paper.

Appendix Nomenclature

Δx_x	positioning error
Δy_x	*Y* direction of straightness error
Δz_x	*Z* direction of straightness error
Δa_x	roll error
$\Delta \beta_x$	pitch error
Δy_x	yaw error
Δx_y	*X* direction of straightness error
Δy_y	positioning error
Δz_y	*Z* direction of straightness error
Δa_y	pitch error
$\Delta \beta_y$	roll error
Δy_y	yaw error
Δx_z	*X* direction of straightness error
Δy_z	*Y* direction of straightness error
Δz_z	positioning error
Δa_z	pitch error
$\Delta \beta_z$	yaw error
Δy_z	roll error
Δx_ψ	*X* direction run-out error
Δy_ψ	*Y* direction run-out error
Δz_ψ	*Z* direction run-out error
$\Delta \alpha_\psi$	around the *X*-axis turning error
$\Delta \beta_\psi$	around the *Y*-axis turning error
$\Delta \gamma_\psi$	turning error
Δx_B	*X* direction run-out error
Δy_B	*Y* direction run-out error
Δz_B	*Z* direction run-out error
$\Delta \alpha_B$	around the *X*-axis turning error
$\Delta \beta_B$	turning error
$\Delta \gamma_B$	around the *Z*-axis turning error
Δx_A	*X* direction run-out error
Δy_A	*Y* direction run-out error
Δz_A	*Z* direction run-out error
$\Delta \alpha_A$	turning error
$\Delta \beta_A$	around the *Y*-axis turning error
$\Delta \gamma_A$	around the *Z*-axis turning error
$\Delta \gamma_{xy}$	*X*, *Y* -axis perpendicularity error
$\Delta \beta_{xz}$	*X*, *Z* -axis perpendicularity error
$\Delta \alpha_{yz}$	*Y*, *Z* -axis perpendicularity error
$\Delta \gamma_{xB}$	*B*-axis parallelism error in the *YZ* plane
$\Delta \alpha_{zB}$	*B*-axis parallelism error in the *XY* plane
$\Delta \gamma_{yA}$	*A*-axis parallelism error in the *XZ* plane
$\Delta \beta_{zA}$	*A*-axis parallelism error in the *XY* plane

References

1. Bohez EL, Ariyajunya B, Sinlapeecheewa C et al (2007) Systematic geometric rigid body error identification of 5-axis milling machines. Int J Comp Aided Des 39(4):229–244
2. Chen JS (1995) Computer-aided accuracy enhancement for multi-axis CNC machine tool. Int J Mach Tools Manuf 35(4):593–605
3. Chen JS, Yuan JX, Ni J et al (1992) Compensation of non-rigid body kinematic effect on a machining center. Tran NAMRI/SME 20:325–329
4. Cheng Q, Zhang ZL, Zhang GJ, Gu PH, Cai LG (2015) Geometric accuracy allocation for multi-axis CNC machine tools based on sensitivity analysis and reliability theory. Proc Inst Mech Eng C J Mech Eng Sci 229(6):1134–1149
5. Fan C, Dong C, Zhang C, Wang HP (2001) Detection of machine tool contouring errors using wavelet transforms and neural networks. J Manuf Syst 20(2):98–112
6. Cai L, Zhang Z, Cheng Q, Liu Z, Gu P, Qi Y (2016) An approach to optimize the machining accuracy retainability of multi-axis NC machine tool based on robust design. Precis Eng 43:370–386
7. Cai L, Zhang Z, Cheng Q, Liu Z, Gu P (2015) A geometric accuracy design method of multi-axis NC machine tool for improving machining accuracy reliability. Eksploatacja i Niezawodnosc-Maint Reliab 17(1):143–155
8. Lunjun C (2005) Genetic algorithm (GA) of mechanical optimization design[M]. China Machine Press, Beijing
9. Ding W, Zhou M, Huang X et al (2007) Study on accuracy design of multi-axis machine tools oriented to remanufacturing. J Basic Sci Eng 4:001–017
10. Lee D-M, Yang SH (2010) Mathematical approach and general formulation error synthesis modeling of multi-axis system. Int J Mod Phys B 24(15):2737–2742
11. Dorndorf U, Kiridena VSB, Ferreira PM (1994) Optimal budgeting of quasistatic machine tool errors. J Eng Ind 116(1):42–53
12. Dong Z, Hu W, Xue D (1994) New production cost-tolerance models for tolerance synthesis. ASME J Eng Ind 116:199–206
13. Dufour P, Groppetti R (1981) Computer aided accuracy improvement in large NC machine-tools. In Proceedings of the 2006 International Conference on the MTDR 22: 611–618
14. Fan JW, Guan JL et al (2002) A universal modeling method for enhancement the volumetric accuracy of CNC machine tools. J Mater Proc Technol 129:624–628
15. Fang HW (2014) The fuzzy neural control and simulation on vehicle active suspension. Chang'an University, Xi'an
16. Ferreira PM, Liu CR (1986) A contribution to analysis and compensation of the geometric error of a machining center. CIRP Ann 35(1):259–262

17. Hocken R, Simpson JA, Borchardt B et al (1977) Three dimensional metrology. J Ann CIRP 26(2):403–408
18. Huang MF, Zhong YR, Xu ZG (2005) Concurrent process tolerance design based on minimum product manufacturing cost and quality loss. Int J Adv Manuf Technol 25(7–8):714–722
19. Huang X, Ding W, Hong R (2006) Research on accuracy design for remanufactured machine tools. In Proceedings of the 2006 International Conference on Technology and Innovation :1403–1410
20. Ni J (1997) CNC machine accuracy enhancement through real-time error compensation. ASME J Manuf Sci Eng 119:717–725
21. Jin S, Zheng C, Yu K, Lai X (2010) Tolerance design optimization on cost–quality trade-off using the Shapley value method. J Manuf Syst 29(4):142–150
22. Khan AW, Chen W (2011) A methodology for systematic geometric error compensation in five-axis machine tools. Int J Adv Manuf Technol 53(5–8):615–628
23. Kiridena VSB, Ferreira PM (1994) Kinematic modeling of quasistatic errors of three-axis machining centers. Int J Mach Tools Manuf 34(1):85–100
24. Kim K, Kim MK (1991) Volumetric accuracy analysis based on generalized geometric error model in multi-axis machine tools. Mech Mach Theory 26(2):207–219
25. Krishna AG, Rao KM (2006) Simultaneous optimal selection of design and manufacturing tolerances with different stack-up conditions using scatter search. Int J Adv Manuf Technol 30(3–4):328–333
26. Liu HL, Li B, Wang XZ et al (2011) Characteristics of and measurement methods for geometric errors in CNC machine tools. Int J Adv Manuf Technol 54:195–201
27. Liu YW, Zhang Q, Zhao XS, Zhang ZF (2002) Multi-body system based technique for compensating thermal errors in machine centers. Chin J Mech Eng 38(1):127–130
28. Liu Y, Li Y (2004) Dimension chain calculation precision in control of hull construction. J Shipbuild China 45(2):81–87
29. Lu Q, Zhang Y (2002) Accuracy synthesis of a hexapod machine tool based on Monte-Carlo method. Chin J Mech Eng 13(6):464–467
30. Love WJ, Scarr. AJ(2006) The determination of the volumetric accuracy of multi-axis machines. In Proceedings of the 2006 International Conference on the 14th MTDR 1973: 307–31
31. Muthu P, Dhanalakshmi V, Sankaranarayanasamy K (2009) Optimal tolerance design of assembly for minimum quality loss and manufacturing cost using metaheuristic algorithms. Int J Adv Manuf Technol 44(11–12):1154–1164
32. Portman VT (1982) A universal method for calculating the accuracy of mechanical devices. J Soviet Eng Res 1(7):11–15
33. Schultschik R (1977) The components of volumetric accuracy. CIRP Ann 25(1):223–228
34. Shen G, Yingzhi Z, Xue Y, Bingkun C, Yu H (2009) Comprehensive evaluation on reliability of numerically-controlled machine tool based on entropy weight method. J Jilin Univ (Eng Technol Ed) 39(5):1208–1211
35. Shin S, Kongsuwon P, Cho B (2010) Development of the parametric tolerance modeling and optimization schemes and cost-effective solutions. Eur J Oper Res 207:1728–1741
36. Khodaygan S, Movahhedy MR, Saadat Foumani M (2011) Fuzzy-small degrees of freedom representation of linear and angular variations in mechanical assemblies for tolerance analysis and allocation. Mech Mach Theory 46:558–573
37. Srivastava A, Veldhuis S, Elbestawi MA (1995) Modeling geometric and thermal errors in a five-axis CNC machine tool. Int J Mach Tools Manuf 35(9):1321–1337
38. Sivakumar K, Balamurugan C, Ramabalan S (2011) Concurrent multi-objective tolerance allocation of mechanical assemblies considering alternative manufacturing process selection. Int J Adv Manuf Technol 53(5–8):711–732
39. Taguchi G (1985) Wu Y. Introduction to off-line quality control. Cent Japan Qual Control Assoc
40. Wang C, Fei Y, Hu P, et al. (2006) Accuracy distribution and determination of the flexible three-coordinate measuring machine[C]// Third International Symposium on Precision Mechanical Measurements. Int Soc Opt Photon 62800U-62800U-7
41. Wang E (1985) An investigation in cyclic optimum method of accuracy allocation for instruments. Chin J Sci Instrum 6(2):140–146
42. Wang SX, Yun JT, Zhang ZF (2003) Modeling and compensation technique for the geometric errors of five-axis CNC machine tools. Chin J Mech Eng 16(2):197–201
43. Xu L, Fan S, Ma Y (2003) Accuracy modeling and error analysis for a new type parallel machine tool. J Sichuan Univ 4:1–5
44. Xu X (2013) Research and application on accuracy distribution and optimization of high-grade CNC machine tools[D]. Zhejiang University, Hangzhou
45. Yang H, Fei Y, Chen X (2006) Uncertainty analysis and accuracy design of Nano-CMM. J Chongqing Univ 29(8):82–86
46. Yang C, Cui Y, Zhao Y (2004) The optimization of main structure parameters in 5-UPS parallel machine tool. Mie China 5:105–110
47. Yang JG, Wang XS, Zhao HT(2005) temperature measurement points optimization selection of machine tools. Chin Mech Eng Soc Ann Conf 627–632
48. Ye B, Salustri FA (2003) Simultaneous tolerance synthesis for manufacturing and quality. Res Eng Des 14(2):98–106
49. Yu ZM, Liu ZJ, Ai YD, Xiong M (2013) Geometric error model and precision distribution based on reliability theory for large CNC gantry guideway grinder. Aust J Mech Eng 49(17):142–151
50. Yu ZM, Liu ZJ, Ai YD, Xiong M (2014) Thermal error modeling of NC machine tool using neural fuzzy control theory. Chinese J Mec Eng 25(16):2224–2231
51. Zhang GJ, Cheng Q, Shao XY et al (2008) Accuracy analysis for planar linkage with multiple clearances at turning pairs. Chinese J Mec Eng 21(2):36–41
52. Zhang X, Chang W, Tan Y (2003) Accuracy allocation of anti-tank missile weapon system. J Proj Rock Miss Guid 23(2):17–19
53. Zhu SW, Ding GF, Qin SF et al (2012) Integrated geometric error modeling, identification and compensation of CNC machine tools. Int J Mach Tools Manuf 52:24–29